

Pion cross section measurements on aligned ^{165}Ho in the (3,3) resonance region*

T. R. Fisher, J. A. Becker, and B. A. Watson

Lockheed Palo Alto Research Laboratory, Palo Alto, California 94304

H. Marshak

Institute for Basic Standards, National Bureau of Standards, Washington, D. C. 20234

G. R. Burleson

New Mexico State University, Las Cruces, New Mexico 88003

M. D. Cooper and D. C. Hagerman

Los Alamos Scientific Laboratory, Los Alamos, New Mexico 87545

I. Halpern

University of Washington, Seattle, Washington 98195

M. J. Jakobson and R. H. Jeppeson

University of Montana, Missoula, Montana 59801

K. F. Johnson

New Mexico State University, Las Cruces, New Mexico 88003

L. D. Knutson

University of Wisconsin, Madison, Wisconsin 53706

R. E. Marrs

California Institute of Technology, Pasadena, California 91109

H. O. Meyer

University of Basel, Basel, Switzerland

R. P. Redwine

Los Alamos Scientific Laboratory, Los Alamos, New Mexico 87545

(Received 8 August 1977)

The removal cross section $\sigma(\Omega)$ for the interaction of π^+ and π^- with aligned ^{165}Ho has been measured at $E_\pi = 115, 165,$ and 240 MeV employing a single crystal holmium target with a nuclear alignment $B_2 = -0.44$. The range of Ω was from 0.05 to 0.55 sr. The data on $\sigma(\Omega)$ and $\Delta\sigma(\Omega)$, the difference between the aligned and unaligned cross sections, are compared with the predictions of a coupled-channels optical model calculation employing parameters from recent muonic x-ray data.

I. INTRODUCTION

further enhanced by the fact that, at the peak of the resonance, calculated cross sections tend to be inde-

* This is the first of a series of papers on this subject.

These considerations have motivated a study of the total cross section for the interaction of pions with aligned ^{165}Ho nuclei in the (3, 3) resonance region. ^{165}Ho is a favorite choice for oriented target experiments since it is monoisotopic and its large hyperfine interaction energy⁹ makes orientation by thermal equilibrium techniques possible at relatively high temperatures. The most reliable measurements of the charge distribution moments come from Coulomb excitation¹⁰ and muonic x-ray data¹¹ which are in good agreement with a quadrupole moment of 7.5 b or, equivalently, a deformation parameter $\beta_2 \approx 0.33$. The hexadecapole moment is less well known, but it is generally conceded to be small; a value of 0.52 b² is obtained from muonic x-ray data.¹¹ The data obtained with oriented ^{165}Ho targets employing proton,¹² α ,¹³ and neutron¹⁴ beams as probes are well explained by assuming that the proton deformation parameters apply to the neutrons as well, but this does not rule out differences of the order of 10–15% which should, in principle, be detectable in a pion total-cross-section experiment. In addition, total-cross-section measurements might be expected to reveal such features as the variation in surface diffuseness proposed on the basis of muonic x-ray¹¹ and electron scattering¹⁵ data.

The experimental technique employed is described in detail in Sec. II, with particular emphasis on the aligned ^{165}Ho target. Section III presents a theoretical analysis of the data employing an ordinary local optical potential model together with the adiabatic coupled-channels formalism as suggested by Silbar and Sternheim.⁵ Comparisons are given with calculations employing the Kisslinger potential in the distorted-wave Born approximation (DWBA) formalism to indicate the degree of model dependence in the theoretical results. Section IV discusses the significance of the data and suggests some possible directions for future experiments.

II. EXPERIMENTAL METHOD

A. Pion beam line and detection system

The experiment was carried out on the low-energy-pion (LEP) channel¹⁶ at LAMPF, and Fig. 1 shows a schematic diagram of the experimental layout. Detector D1 is a scintillator used to reject multiple-pion events, detectors D2, D7, and D8 are thin scintillation counters which provide the geometrical definition of the beam, and D3

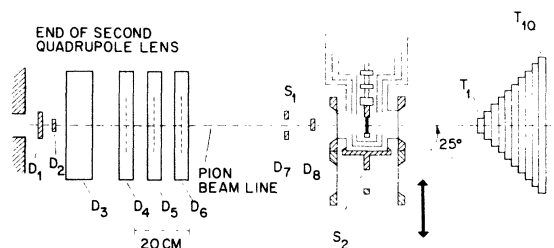


FIG. 1. Schematic diagram of experimental arrangement. D1, multiple event rejector; D2, D7, D8, beam defining counters; D3, DISC Cerenkov counter; D4, D5, D6, multiwire proportional counters; S1, holmium target; S2, blank target; T1–T10, scintillator stack.

signals from D1, D2, D3, D7, and D8, and typical average counting rates were of the order 10^3 good pion events/sec. The subsequent removal of a tagged pion from the beam by interaction in the ^{165}Ho target was detected by the series of concentric circular scintillation counters of increasing diameter designated as T1–T10 in Fig. 1. The recorded data consisted of coincidences between a good pion event and different combinations of T1 through T10. All operations involving data recording and storage were controlled by an on-line PDP-11/45 computer.

The pion detection apparatus was the product of an extensive developmental effort, and has been employed in the measurement of numerous other total cross sections. A more complete description of the apparatus will accompany the publication of several papers which are currently in preparation.

B. Aligned ^{165}Ho target

The crystal structure of holmium metal is hexagonal-close-packed, and at low temperatures the atomic magnetic moments form a spiral structure about the c axis with individual moments canted at an angle of $\pm 10^\circ$ with respect to the basal plane.¹⁸ Cooling a single crystal of the metal to temperatures where kT is comparable to the energy of the hyperfine interaction between the $4f$ electrons and the atomic nucleus results in a nuclear alignment which has the c axis as an axis of symmetry. Only the even-rank orientation tensors¹⁹ are nonzero, and the normalized second-rank tensor B_{20} , written hereafter as B_2 , has the value $-0.46 [P_2(80^\circ)]$ at zero temperature. This corresponds to almost complete alignment of the nuclear spin axis perpendicular to the beam direction. It is thus possible to construct target for cross-section mea-

periment consisted of two slabs cut perpendicular to the c axis from a large single crystal.²¹ These slabs were soldered to a 3.6-cm i.d. copper ring which was attached to the mixing chamber of a ^3He - ^4He dilution refrigerator. Cd-Bi eutectic solder was used for all joints. The target had a useful diameter just under 3.6 cm and an average thickness of 1.02 mm, with a seam running through the center (which did not materially affect the cross-section measurements). The target size allowed a margin of about 7 mm between the edge of the beam spot and the copper ring, so alignment of the target was not critical. Calibrated carbon resistors,²² attached to each half of the holmium target and also to the copper support ring, served as temperature monitors.

Before soldering, the two halves of the target were spark-planed to uniform thickness and chemically polished. X-ray diffraction patterns were recorded at 16 separate points on the target surface after soldering to check the alignment of the crystal axes and to inspect the surface for damage resulting from the cutting and soldering operations. These patterns, as well as earlier ones taken during the spark cutting operations, were all of excellent quality, demonstrating clearly that the target was a good single crystal. The error in alignment of the crystal axes on the basis of these x-ray patterns was estimated to be $<1^\circ$ and any surface damage was confined to a thickness $<2.5 \mu\text{m}$.

The dilution refrigerator system which was used to cool the holmium target was of standard design and similar in most respects to a system described previously for use with a polarized ^{59}Co target.²³ The external Dewar windows were 25- μm Havar foil, and 25- and 25- μm Al foil was employed on the thermal radiation shields. In all, the total scattering material in the path of the beam included 42 mg/cm² of Havar and 22 mg/cm² of Al in addition to the 890 mg/cm² represented by the holmium target itself. The lowest temperature of the refrigerator in absence of a heat load was below 0.03 K, but no effort was made to reach very low temperatures since the nuclear alignment in ^{165}Ho is almost at its maximum value at 0.08 K. This temperature was reached approximately $1\frac{1}{2}$ hours after starting the ^3He - ^4He circulation from a temperature of 1.5 K, and a small amount of heat was then applied to the mixing chamber to stabilize its temperature. The heating coil wrapped about the mixing chamber also made it possible to warm the target rapidly from 0.08 to 1.5 K to begin the "warm target" part of a run cycle.

The calculated values of the nuclear alignment are $B_2 = -0.44$ at 0.08 K and $B_2 = -0.02$ at 1.5 K giving a net difference $B_2 = -0.42 \pm 0.02$. The val-

ues $a' = 0.32$ K and $p = 0.06$ K were chosen for the hyperfine coupling parameters based on a consensus of data from several authors.⁹ The quoted uncertainty includes uncertainty in the temperature of the target due to possible beam heating effects as well as uncertainties in the resistor calibration, alignment of crystal axes, and hyperfine parameters.

C. Procedure for recording data

It is standard procedure in total-cross-section measurements to make frequent comparisons between the target and a reference blank target which has the same support structure. The removal of particles attributed to the target is determined by subtraction, and the frequent cycles tend to eliminate systematic errors from long-term drifts in the electronics or the beam parameters. In the present experiment, the blank target assembly was suspended from the bottom of the dewar which housed the aligned target (see Fig. 1). Dummy frames and foils were provided to simulate the Dewar windows, as well as an identical copper target holder with the holmium crystal omitted. The blank target was alternated with the real one at intervals of about two minutes, and the apparatus for moving the targets was controlled automatically by the PDP 11/45 computer with the interchange being effected upon the accumulation of a predetermined number of pion events. The accuracy of the blank subtraction was checked by comparing the results against a cross-section measurement made in more conventional geometry where the extraneous mass around the target was kept small. The results were in agreement within the statistical accuracy (3%) of the measurements.

Comparison between the aligned and unaligned states of the target was made by cycling the target between a temperature of 0.08 K ($B_2 = -0.44$) and a temperature of 1.5 K ($B_2 = -0.02$). Such cycles should affect no target parameters other than the nuclear alignment in a systematic way. A typical measurement began with about three hours of running with the holmium target at 1.5 K during which time approximately 5×10^6 pions were recorded for both the target and blank. This was followed by a $1\frac{1}{2}$ hour cool-down to 0.08 K and 6 hours of running to obtain 10^7 recorded pion events. The target was then warmed in a few minutes to 1.5 K and an additional 5×10^6 events recorded.

The raw data were reduced to cross sections $\sigma(\Omega_i)$ corresponding to removal of a pion from the solid angle Ω_i subtended by the i th detector. Subtraction of the 1.5-K results from the 0.08-K results then gives the corresponding values of $\Delta\sigma(\Omega_i)$ which results from the nuclear alignment in the target. The usual procedure is to correct

for Coulomb effects and extrapolate to $\Omega=0$ in an attempt to obtain an essentially model independent total cross section.²⁴ However, in the case of a heavy nucleus, the Coulomb effects are large and the differential cross section strongly forward-peaked, which makes the validity of the usual analysis procedure questionable. One way out of this difficulty has been proposed by Cooper and Johnson.²⁵ In this paper, we adopt an alternative approach of a direct theoretical fit to the experimental values of $\sigma(\Omega)$ and $\Delta\sigma(\Omega)$. This analysis is described in the following section.

III. DATA ANALYSIS

A. Theoretical calculations

The removal cross section $\sigma(\Omega)$ [or $\Delta\sigma(\Omega)$] which is derived from the raw data is the cross section for removal of a pion from solid angle Ω and is given by

$$\sigma(\Omega) = \sigma_a(\Omega) + \int_{\Omega}^{4\pi} \text{Tr} \rho F F^\dagger d\Omega'. \quad (3.1)$$

The first term on the right is the contribution from reactions and inelastic scattering and the second term represents the elastic scattering contribution. ρ is the density matrix which describes the orientation state of the target and F is the total elastic scattering amplitude. Equation (3.1) may also be written in the form

$$\begin{aligned} \sigma(\Omega) = & \sigma + \int_{\Omega}^{4\pi} \text{Tr} \rho (F F^\dagger - F_N F_N^\dagger) d\Omega' \\ & - \int_{\Omega}^{\Omega} [\text{Tr} \rho F_N F_N^\dagger + \sigma_{\text{inel}}(\theta')] d\Omega', \quad (3.2) \\ \sigma = & \sigma_a + \int_{\Omega}^{4\pi} \text{Tr} \rho F_N F_N^\dagger d\Omega', \end{aligned}$$

$$F = F_C + F_N,$$

where F_C is the Coulomb amplitude, F_N is the nuclear amplitude, and $\sigma_{\text{inel}}(\theta)$ is the inelastic differential cross section. (The contribution of this term was assumed to come entirely from the first two excited states of the ground state rotational band in the case of ¹⁶⁵Ho.)

The preceding equation may be employed to extract the total cross section σ from data on $\sigma(\Omega)$. The usual procedure is to calculate the second term on the right, which contains all Coulomb effects, subtract it from $\sigma(\Omega)$, and extrapolate the result to $\Omega=0$. A simple extrapolation procedure works well provided that the region where $F_C \geq F_N$ is confined to small values of Ω where the contribution of the third term on the right side of equation (3.2) is small, e.g., in the case of light nuclei with $Z \leq 20$.

An extrapolation procedure which is also appli-

cable to heavy nuclei has been proposed by Cooper and Johnson,²⁵ and an analysis of the data on $\sigma(\Omega)$ from this experiment is currently in progress utilizing this approach. It is hoped that this analysis will provide accurate absolute values of the total cross section σ . The purpose of the present paper is primarily to present the results for $\Delta\sigma(\Omega)$, and for this purpose we have chosen to fit the data directly, evaluating the right side of equation (3.2) by a theoretical calculation. The reasons for this choice will be discussed in more detail at the end of the analysis. For the present, we observe that such an approach, although model dependent, may still provide useful information in the (3,3) resonance region where different models have been shown to give substantially the same results for pion cross sections.⁷

The evaluation of equation (3.2) is conveniently accomplished by employing an optical theorem for σ which is a generalized form of Eq. (15) of Ref. 25:

$$\sigma = \frac{4\pi}{K} \text{Im Tr} \rho \tilde{F}_N(0). \quad (3.3)$$

The amplitude \tilde{F}_N differs from F_N only in its explicit dependence on the Coulomb phase shifts σ_i :

$$\begin{aligned} [F_N(\theta)]_{M, M'} &= \sum_{I I'} e^{i(\sigma_I + \sigma_{I'})} f_{M M', I I'}(\theta), \\ [\tilde{F}_N(\theta)]_{M, M'} &= \sum_{I I'} e^{i(\sigma_I - \sigma_{I'})} f_{M M', I I'}(\theta). \end{aligned} \quad (3.4)$$

The elastic scattering amplitude F and the inelastic cross section $\sigma_{\text{inel}}(\theta)$ may be calculated from an optical model, and two possibilities present themselves here. The Kisslinger potential³ is commonly employed in optical model calculations of pion scattering in the (3,3) resonance region, but because of the complicated nature of this potential it has not been incorporated into a coupled-channels code. Calculations of pion scattering from nonspherical nuclei must therefore treat the nonspherical part of the potential by a perturbation approach such as the distorted-wave Born approximation (DWBA). Alternatively, Silbar and Sternheim⁵ have suggested the use of an ordinary local optical potential with a variable effective radius which permits calculations to be done with existing coupled-channels codes. Such a potential may be written

$$V = - \frac{(\hbar c)^2 A k^2}{2E} (b_0 + b_1) \rho(r), \quad (3.5)$$

$$\int \rho(r) d\vec{r} = 1,$$

where b_0 and b_1 are the usual Kisslinger parameters.

We have adopted the suggestion of Silbar and Sternheim⁵ for the present data analysis because the coupled-channels approach should be more correct in its treatment of the geometrical features of the nucleus. However, a comparison between coupled-channels calculations with an ordinary optical potential and the DWBA-Kisslinger approach shows very similar results for typical cases, as indicated in Figs. 2 and 3. The DWBA expression for σ which was used to calculate the curve in Fig. 2 is derived in Appendix I, and the DWBA results for the differential cross section $\sigma(\theta)$ and $\Delta\sigma(\theta)$ in Fig. 3 were reproduced from published calculations of Iverson and Rost.²⁶ Over the range of energies covered in the present experiment, the values of σ in Fig. 2 are in agreement within 5% and values for $\Delta\sigma$ agree within 15%. Differences in $\sigma(\theta)$ and $\Delta\sigma(\theta)$ are small out to about 20° , and by this time the contribution to the removal cross section $\sigma(\Omega)$ is almost negligible. It seems reasonably certain, therefore, that the DWBA-Kisslinger approach would not differ from the present one

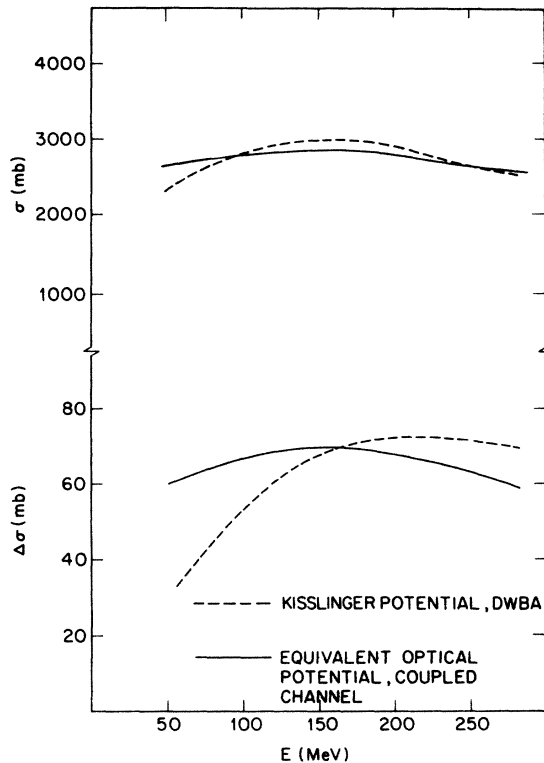


FIG. 2. Calculated curves of the total cross section σ and the difference in aligned and unaligned total cross sections $\Delta\sigma$ for positive pions incident on ^{165}Ho . The nuclear alignment is $B_2 = -0.42$. The calculations were performed with the geometrical parameters of Ref. 26: $R_0 = 5.7$ fm, $\beta_2 = 0.33$, $\beta_4 = 0$, $a = 0.605$ fm. The DWBA expression for $\Delta\sigma$ is given in Appendix A.

by more than 5% in $\sigma(\Omega)$ or 15% in $\Delta\sigma(\Omega)$. This degree of model independence is reassuring, in view of the very significant differences in the two models, and is consistent with other observations of model independence in the (3, 3) resonance region.⁷

For the present data analysis, a proton coupled-channels code employing the adiabatic approximation was modified to solve an approximate Klein-Gordon equation of the form

$$(-\nabla^2 + \mu^2)\psi \approx [E^2 - 2E(V + V_c)]\psi, \quad (3.6)$$

where μ is the mass and V_c is the Coulomb potential. The criterion for validity of the adiabatic approximation,²⁷ that the energy of the scattered particle be large in comparison with the energy separation of levels in the ground state rotational band, is well satisfied in the present case. Values of b_0 and b_1 in expression (3.5) for V were derived from the energy-averaged pion-nucleus amplitudes of Sternheim and Auerbach.²⁸ In the case of a nucleus as heavy as ^{165}Ho , the energy dependence of the effective radius in the model of Silbar and Sternheim⁵ is negligible. The deformed nuclear matter distribution was assumed to have the form

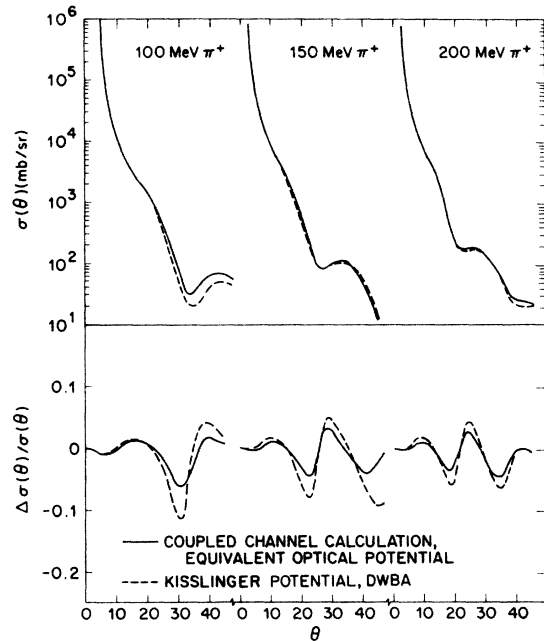


FIG. 3. Calculated curves of the differential cross section, $\sigma(\theta)$, and the difference between aligned and unaligned differential cross sections, $\Delta\sigma(\theta)$, for positive pions incident on ^{165}Ho . The Kisslinger-DWBA curves were reproduced from Ref. 26 and scaled to a nuclear alignment $B_2 = -0.42$. The geometrical parameters are also those of Ref. 26.

$$\rho(r, \theta) = \rho_0 \left[1 + \exp\left(\frac{r - R(\theta)}{a}\right) \right]^{-1}, \quad (3.7)$$

$$R(\theta) = R_0 [1 + \beta_2 Y_2(\theta) + \beta_4 Y_4(\theta)]$$

and the geometrical parameters were taken from recent muonic x-ray data¹¹:

$$\begin{aligned} R_0 &= 6.14 \text{ fm}, \\ \beta_2 &= 0.322, \\ \beta_4 &= 0.040, \\ a &= 0.49 \text{ fm}, \\ R_{0c} &= 6.14 \text{ fm}, \end{aligned} \quad (3.8)$$

R_{0c} is the Coulomb radius, and the Coulomb potential was taken to be that of a uniformly charged prolate spheroid with deformation β_2 .

B. Results

The results of the fits to $\sigma(\Omega)$ and $\Delta\sigma(\Omega)$ are presented in Figs. 4 and 5. These fits involve no free parameters, and the strongly correlated nature of the data should be kept in mind when evaluating the goodness of fit. The discrepancy between the experimental and theoretical values of $\sigma(\Omega)$ at small values of Ω is at least partially attributable to multiple scattering. Note that, in the case of $\Delta\sigma(\Omega)$, the usual multiple scattering cor-

rection does not appear since it is independent of nuclear alignment and cancels when the subtraction is performed. For $\Omega > 0.2$ sr, the fits are reasonably good. In this region, $\sigma(\Omega)$ is dominated by the contribution from $\sigma_a(\Omega)$ in Eq. (3.1) since the elastic scattering is strongly forward peaked.

The fits to the $\Delta\sigma(\Omega)$ data are very good at 165 MeV, near the peak of (3,3) resonance, where the data indicate a small but statistically significant effect of about 50 mb. At the other two energies the data tend to be systematically less than the theoretical prediction and are consistent with zero, although the theoretical curves are similar to those at 165 MeV. Because of statistical uncertainties in the data, however, it is impossible to determine whether the calculation fails at energies off the (3,3) resonance or whether the entire body of data should be treated as consistent and averaged. The second interpretation leads, for example, to a value of $\Delta\sigma(\Omega) = 22 \pm 10$ mb at $\Omega = 0.5$ sr which differs significantly from the theoretical prediction of 48 mb, and could imply that some modification is needed in the description of the deformed nuclear matter distribution.

In principle, it should be possible to apply Coulomb corrections to the data and extrapolate to zero solid angle to obtain estimates of $\Delta\sigma$. This was the first approach actually tried, and it led

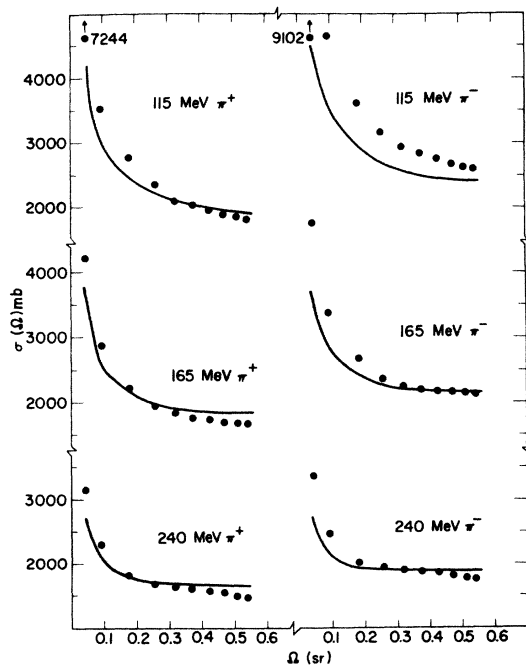


FIG. 4. Experimental data on the removal cross section $\sigma(\Omega)$ from the present experiment with theoretical curves from the coupled-channels calculation described in Sec. III. [The data from which this figure was constructed are available from PAPS (Ref. 31).]

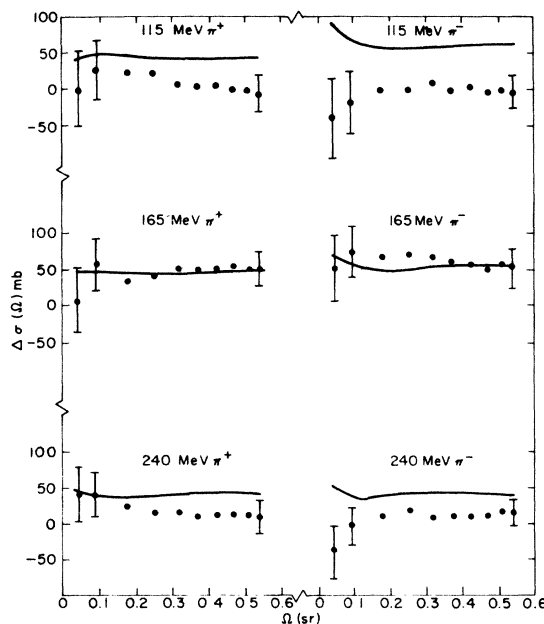


FIG. 5. Experimental data on $\Delta\sigma(\Omega)$, the difference between the aligned, and unaligned values of $\sigma(\Omega)$. The theoretical curves were obtained with the coupled-channels calculation described in Sec. III. [The data from which this figure was constructed are available from PAPS (Ref. 31).]

in most cases to small or negative values of $\Delta\sigma$ because of the downward trend of the first two points in five out of the six cases. This downward trend is not understood and is not reflected in any of the calculated curves. We suspect that it may not indicate a real cross-section trend, however, because it would imply that the alignment effect on the forward elastic cross section is opposite in sign from the geometrical effect. For a nucleus which must bear strong resemblance to a totally absorbing black spheroid, this would be difficult to explain. We have therefore preferred to present the entire body of data on $\Delta\sigma(\Omega)$ together with the theoretical curves.

Finally, we may ask how sensitive the present experiment is to an angular variation in the diffuseness of the nuclear surface or to a difference in the neutron and proton deformation parameters. A variation in surface diffuseness can be introduced by allowing the parameter a in equation

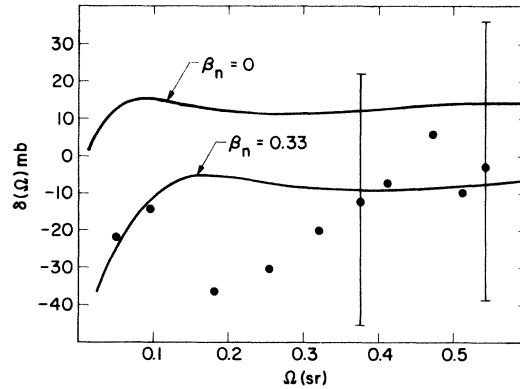


FIG. 7. Calculated curves of $\delta(\Omega)$, the difference between $\Delta\sigma(\Omega)$ for positive and negative pions, at 165 MeV illustrating the effect of varying the neutron deformation parameter β_{2n} while fixing the proton deformation parameter at 0.33. The data are from the present experiment.

the plane of scattering and perpendicular to it, as in the two electron-scattering experiments on a aligned ^{165}Ho carried out at Stanford University.²⁹ An experiment conceived along these lines has been proposed for the EPICS channel at LAMPF.

The possibility of employing high-energy beams in experiments with aligned targets to study A -dependent effects has been suggested by Goldhaber.³⁰ Presumably, one might distinguish between multiple successive processes and processes requiring the cooperative interaction of several neighboring nucleons by studying cross sections corresponding to different orientations of a deformed nucleus. The present experiment clearly establishes the feasibility of performing such experiments in the immediate future.

ACKNOWLEDGMENTS

We would like to thank Mr. B. Beaudry and Dr. Dr. K. A. Gschneider of the Ames Research Laboratory for supplying the large holmium crystal from which the target was cut, Mr. R. B. Dove for his technical help in preparing the target, and the

technical staff at the Los Alamos Meson Physics Facility for their support during the course of the experiment. We were assisted in our interpretation of the data by helpful conversations with Professor D. H. Wilkinson.

APPENDIX A. DWBA EXPRESSION FOR $\Delta\sigma$

The scattering amplitude F_N may be written as the sum of two parts

$$F_N = F_0 + F_1, \quad (\text{A1})$$

where F_0 is the spin-independent part. The spin-dependent part may be calculated in the distorted-wave Born approximation

$$(F_1)_{M'M} = -\frac{1}{4\pi} \frac{2E}{(\hbar c)^2} \times \int \chi^{(-)*}(\vec{r}) \langle M' | U^{(1)} | M \rangle \chi^{(+)}(\vec{r}) d^3\vec{r}, \quad (\text{A2})$$

where $U^{(1)}$ is the spin-dependent part of the scattering potential. For the Kisslinger potential in the case of a nucleus with quadrupole deformation parameter β_2 ,

$$\frac{2E}{(\hbar c)^2} \langle M' | U^{(1)} | M \rangle = \beta_2 A (IM2m | IM') (IK20 | IK) \{ -b_0 k^2 F(r) Y_2^m(r) + b_1 \vec{\nabla} \cdot [F(r) Y_2^m(\hat{r}) \vec{\nabla}] \},$$

$$F(r) = R_0 \left. \frac{\partial \rho}{\partial R} \right|_{R=R_0}. \quad (\text{A3})$$

Plugging in the usual expansions for the distorted waves $\chi^{(-)}$ and $\chi^{(+)}$ and using equations (3.3) and (3.4) of Sec. III leads to the result

$$\Delta\sigma(\text{DWBA}) = -\frac{(20\pi)^{1/2} A \beta_2 B_2 I(2I-1)}{k^3 (I+1)(2I+3)} \text{Im} \sum_{l'l'} i^{l-l'} e^{i(\sigma_l - \sigma_{l'})} (2l+1)(2l'0 | l'0)^2 I_{l'l}, \quad (\text{A4})$$

where

$$I_{l'l} = -b_0 k^2 G_I - b_1 G_{II} + b_1 G_{III} \Delta_{l'l}. \quad (\text{A5})$$

Expressions for G_I , G_{II} , G_{III} , and $\Delta_{l'l}$ are given in Ref. 26, and b_0 and b_1 are the usual Kisslinger parameters.

*Work supported in part by the Lockheed Independent

- ¹¹R. J. Powers, F. Boehm, P. Vogel, A. Zehnder, T. King, A. R. Kunselman, P. Roberson, P. Martin, G. H. Miller, R. E. Welsh, and D. A. Jenkins, *Phys. Rev. Lett.* **34**, 492 (1975).
- ¹²T. R. Fisher, S. L. Tabor, and B. A. Watson, *Phys. Rev. Lett.* **27**, 1078 (1971).
- ¹³D. R. Parks, S. L. Tabor, B. B. Triplett, H. T. King, T. R. Fisher, and B. A. Watson, *Phys. Rev. Lett.* **29**, 1264 (1972).
- ¹⁴H. Marshak, A. Langsford, T. Tamura, and C. Y. Wong, *Phys. Rev. C* **2**, 1 (1970).
- ¹⁵T. Cooper, W. Bertozzi, J. Heisenberg, S. Kowalski, W. Turchinets, C. Williamson, L. Cardman, S. Fiv-
zinsky, J. Lightbody, Jr., and S. Penner, *Phys. Rev. C* **13**, 1083 (1976).
- ¹⁶R. L. Burman, R. Fulton, and M. Jakobson, *Nucl. Instrum. Methods* **131**, 29 (1975).
- ¹⁷B. A. Leontic and J. Teiger, Brookhaven National Laboratory Report No. BNL 50031, 1966 (unpublished).
- ¹⁸W. C. Koehler, J. W. Cable, E. O. Woolan, and M. K. Wilkinson, *J. Phys. Soc. Jpn. Suppl.* **17**, B-III, 32 (1962); W. C. Koehler, *J. Appl. Phys.* **36**, 1078 (1965).
- ¹⁹The orientation tensors are defined in D. M. Brink and G. R. Satchler, *Angular Momentum* (Clarendon, Oxford, 1962), although a different notation, ρ_{KQ} instead of B_{KQ} , is employed.
- ²⁰H. Marshak, A. C. B. Richardson, and T. Tamura, *Phys. Rev.* **150**, 996 (1966).
- ²¹The holmium crystal was obtained from Ames Laboratory, Iowa State University.
- ²²The use of these resistors for temperature measurements is described by W. C. Black, Jr., W. R. Roach, and J. C. Wheatley, *Rev. Sci. Instrum.* **35**, 587 (1964).
- ²³T. R. Fisher, D. C. Healey, D. Parks, S. Lazarus, J. S. McCarthy, and R. Whitney, *Rev. Sci. Instrum.* **41**, 684 (1970).
- ²⁴J. P. Stroot, Experiments in Pion-Nucleus Physics, in Lectures from the LAMPF Summer School on the Theory of Pion-Nucleus Scattering, 1973, edited by W. R. Gibbs and B. F. Gibson (unpublished).
- ²⁵M. D. Cooper and M. B. Johnson, *Nucl. Phys. A* **260**, 352 (1976).
- ²⁶M. S. Iverson and E. Rost, *Phys. Rev. C* **12**, 1589 (1975).
- ²⁷R. C. Barrett, *Nucl. Phys.* **51**, 27 (1964).
- ²⁸M. M. Sternheim and E. H. Auerbach, *Phys. Rev. C* **4**, 1805 (1971).
- ²⁹R. S. Safrata, J. S. McCarthy, W. A. Little, M. R. Yearian, and R. Hofstadter, *Phys. Rev. Lett.* **18**, 667 (1967); F. J. Urhane, J. S. McCarthy, and M. R. Yearian, *ibid.* **26**, 578 (1971).
- ³⁰M. Goldhaber, in Proceedings of the International Topical Conference on Meson Nuclear Physics, Pittsburgh, Pennsylvania, May, 1976 (unpublished), p. 278.
- ³¹See AIP document No. PAPS PRVCA-16-2367-2 for two pages of tabulated data from which Figs. 4 and 5 were constructed. Order by PAPS number and journal reference from American Institute of Physics, Physics Auxiliary Publication Service, 335 East 45th Street, New York, N. Y. 10017. The price is \$1.50 for microfiche or \$5.00 for photocopies. Airmail additional. Make checks payable to the American Institute of Physics. This material also appears in *Current Physics Microfilm*, the monthly microfilm edition of the complete set of journals published by AIP, on the frames immediately following this journal article.